The paper was published in the proceedings of the 11th International Conference on Physical Modelling in Geotechnics (ICPMG2026) and was edited by Ioannis Anastasopoulos. The conference was held from June 8th to June 12th 2026 in Zurich, Switzerland.

Shaking table tests on a transportation hub combining underground stations and aboveground structures

Z. Zhang
College of Civil Engineering, Tongji University, Shanghai, China, 2410078@tongji.edu.cn

X. Liu
College of Civil Engineering, Tongji University, Shanghai, China, xian.liu@tongji.edu.cn

C. Liu
Architectural Design & Research Institute of Tongji University (Group) Co., Ltd, Shanghai, China, Liuchuanping@126.com

X. Yao
College of Civil Engineering, Tongji University, Shanghai, China, xupengyao@163.com

Y. Yuan
State-Key Laboratory of Disaster Reduction in Civil Engineering, Shanghai, China, yuany@tongji.edu.cn

ABSTRACT: With the continuous advancement of the station-city integration concept, integrated air-rail transportation hubs have emerged as a major innovation in urban transportation infrastructure. This paper investigates the seismic performance of a transportation hub that combines underground stations and aboveground structures through 1g shaking table tests. Based on the dynamic equilibrium equations, similitude relations for shaking table testing were derived. A displacement scaling factor different from the geometry scaling factor was adopted, with particular emphasis on the dynamic response characteristics of the structure within the elastic range. The experimental results reveal pronounced spatial variability in the seismic response of the integrated hub. Under seismic excitation, the dynamic vibration of the aboveground structures leads to amplified acceleration responses in the corresponding underground components compared with those in the purely underground segment. A similar amplification trend is observed in the inter-story relative displacement, with the peak value in the terminal segment reaching up to 3.1 times that of the station-only segment. However, this amplification effect diminishes with increasing burial depth. At the base slab elevation, the spectral response of the underground station in all segments closely matches that of the surrounding soil, indicating that the dynamic behavior is predominantly controlled by site effects. These findings highlight that spatial variability should be adequately considered in the seismic design of integrated transportation hubs.

1 INTRODUCTION

To facilitate convenient transfers among different transportation methods, comprehensive transportation hubs integrating underground railway and metro stations, airport terminals and general transit centers have become key components of modern urban infrastructure (Liu et al., 2018). Within such hubs, underground and aboveground structures are directly connected, forming an integrated and highly complex structural system. Under seismic conditions, however, the overall seismic behavior of the integrated hub system may differ substantially from that of the isolated underground or aboveground structures, owing to irregular stiffness distributions and discontinuous boundary conditions.

Several existing studies have investigated the seismic interaction between underground and aboveground structures within an integrated system through numerical simulations (Li et al., 2023, Qiu et al. 2023). Compared with numerical approaches, physical model tests can provide more intuitive and direct insights into the complex dynamic interactions involved in soil-structure systems (Wu et al., 2020, Yuan et al., 2025). However, due to the large scale and high complexity of comprehensive transportation hubs, few researchers have conducted shaking table tests on the soil-integrated hub systems. In this study, a series of large-scale shaking table tests were designed and implemented on a newly built transportation hub considering the soil-structure interaction. The similitude relations for the ground and the structure were derived based on the dynamic equilibrium equations. To ensure the feasibility of the tests, a displacement scaling factor different from the geometry scaling factor was adopted, and the analysis of the test results was therefore confined to the elastic response range. The experimental results demonstrate that the seismic response within the integrated hub system exhibits significant spatial variability.

2 SHAKING TABLE TESTING

2.1 Testing facilities

The 1-g shaking table tests were conducted using the multi-functional shaking table system at Tongji University. A 10.1 m×6.1 m combined shaking table with a total load capacity of 140 ton was utilized in the testing. The table has three degrees-of-freedom in the horizontal plane, i.e., transverse, longitudinal, and rotational. The maximum output acceleration with full payload capacity can reach ±1.5 g for the frequency range of 0.1-50 Hz. As shown in Figure 1, a laminar box was designed for the shaking table tests, with the external measurements of 10.1 m (length)×6.1 m (width)×1.4 m (height). It is composed of 10 stacked layers of steel frames and each layer can move smoothly along the input direction, thus replicating the ground's layered shear deformation characteristics.

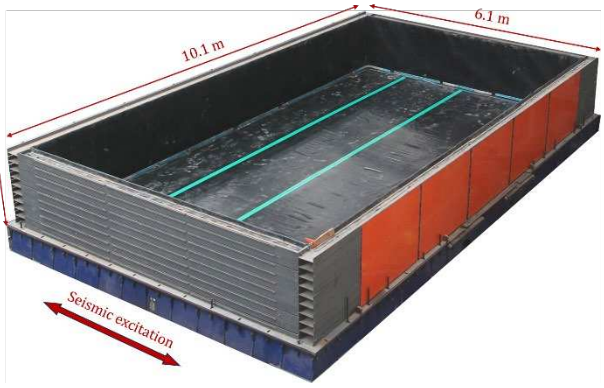

Figure 1. Laminar box used in the shaking table testing

2.2 Similitude relations

The equation of motion for a linear-dynamic system are a set of second-order differential equations. Let $\boldsymbol{M}$, $\boldsymbol{C}$, $\boldsymbol{K}$ be the mass, damping and stiffness matrices, respectively. The state equations can be expressed as:

$$\boldsymbol{M}\ddot{\boldsymbol{u}} + \boldsymbol{C}\dot{\boldsymbol{u}} + \boldsymbol{K}\boldsymbol{u} = \boldsymbol{F}(t) \tag{1}$$

where: $\ddot{\boldsymbol{u}}$, $\dot{\boldsymbol{u}}$ and $\boldsymbol{u}$ are vectors of acceleration, velocity and displacement of the structure, respectively; $\boldsymbol{F}(t)$ is the external force. In the model test, it is first necessary to ensure that the vibration characteristics of the model structure are consistent with those of the prototype, that is, the similarity between the structural inertial forces and the elastic restoring forces should be maintained. Accordingly, the following can be derived:

$$S_\rho \cdot S_l^3 \cdot S_a = S_E \cdot S_l \cdot S_u \tag{2}$$

where: S_ρ, S_l, S_a, S_E, and S_u are scaling factors for density, length, acceleration, elastic modulus, and displacement, respectively. In the shaking table testing, considering the simulation scope of the prototype project and the operating space of the container, the geometry scaling factor (from prototype to model) is selected as $S_l = 1/40$. Since the experiments are conducted at 1-g environment, the acceleration scaling factor is set to $S_a = 1$. Moreover, organic glass is chosen as the material of the model structure, and the scaling factor for elastic modulus is then determined to be $S_E = 1/10.5$.

Within the range of small elastic deformations, the structural displacement response follows the superposition principle, i.e. $u = \sum_n u_n(t)$. This allows independent selection of the displacement scaling factor despite the value of the geometry scaling factor (Lin et al., 2000). As demonstrated by Eq. (2), adopting a smaller displacement scaling factor can reduce the target equivalent density of the model structure, thereby effectively decreasing the amount of required additional mass. Consequently, a displacement scaling factor of $S_u = 1/100$ was selected, yielding a corresponding density scaling factor of $S_\rho = 1.5$. After modification, the mass of the counterweights was reduced to twice the model station's self-weight. It should be noted that the scaling factors for time, frequency, and velocity were also adjusted correspondingly with the change in the displacement scaling factor. The adjusted similarity relations adopted in the testing are summarized in Table 1.

Table 1. Design of similitude relations

Physical quantity	Similarity relation	Scaling factor
Length l	S_l	1/40
Displacement u	S_u	1/100
Acceleration a	S_a	1
Time t	$S_t = S_u^{1/2} S_a^{-1/2}$	1/10
Frequency ω	$S_\omega = S_t{}^{-1}$	1/0.1
Elastic modulus E	S_E	1/10.5
Density ρ	$S_\rho = S_E S_l^{-2} S_u S_a^{-1}$	1/0.66
Mass m	$S_m = S_\rho S_l^3$	1/42000

2.3 Model design

2.3.1 Model structure

The prototype is an integrated complex comprising a T3 airport terminal, a general transit center (GTC), and two underground rail transportation systems. Both the T3 terminal structure and the GTC structure adopt reinforced concrete frame structural systems and consist of combined aboveground and underground components. The high-speed railway and metro lines are constructed beneath the GTC and T3 structures, with stations built synchronously with the superstructures. The design scope of the prototype airport and the regional structural layout are illustrated in Figure 2. Along the longitudinal direction, the study area can be divided into the GTC segment, the station segment, and the T3 terminal segment.

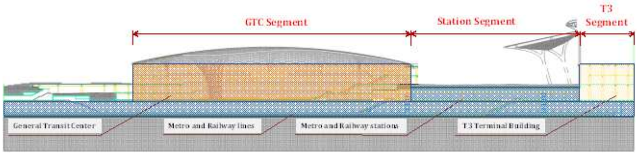

Figure 2. Regional structural layout of the prototype transportation hub

Under seismic excitation, above-ground and underground structures exhibit markedly different dynamic response mechanisms (Tsinidis, 2016). For underground stations, the relative stiffness between the structure and the surrounding soil is one of the key parameters governing soil-structure interaction behavior, whereas for aboveground structures, the dynamic response characteristics are primarily controlled by the structural modal parameters. To ensure that the overall dynamic response of the integrated hub system meets the requirements of similarity, numerical simulations were employed in this study to independently verify the consistency of the stiffness of the underground stations and the modal parameters of the above-ground structures, both in prototype and model scales.

In shaking table tests of underground structures, granular concrete is commonly used to simulate prototype reinforced concrete structures (Wu et al., 2020). However, due to the large spatial scale of the hub structure and the complexity of its structural layout, it would be difficult to ensure fabrication precision using granular concrete casting. In this study, organic glass was utilized as the material for the manufacturing of the model structure. As summarized in former publications (Chen et al., 2016, Cheng et al., 2023), this material has good homogeneity, high strength and low elastic modulus, and is also suited for accurately manufacturing. Taking the underground station as an example, each station segment of the model was fabricated by separately manufacturing the roof slab, base slab, sidewalls, longitudinal beams, and central columns, which were then assembled using epoxy resin with a prescribed mixing ratio, as illustrated in Figure 3.

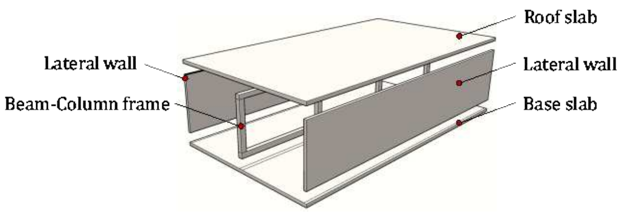

Figure 3. Manufacture of the model station

After the integrated structural model was completed, counterweights were uniformly distributed on the surfaces of each floor in accordance with the equivalent density similarity ratio determined in Section 2.2. Specifically, the density of the model structure obtained from the similarity analysis is 3640 kg/m³, whereas the actual density of the plexiglass is 1200 kg/m³. Therefore, an additional equivalent mass equal to twice the original model mass was required, in order to ensure similarity in the equivalent mass between the model structure and the prototype structure. The assembled model structure in the shaking table testing is presented in Figure 4.

Figure 4. Assembled model hub structure

2.3.2 Model soil

The prototype site depth simulated in the experiment is 54 m. To compensate for the scale effects induced by model scaling, a model soil composed of sawdust and sand mixed in a specified proportion was adopted to simulate the prototype strata. By adjusting the mass ratio of sawdust to sand, the dynamic properties of the model soil can be effectively modified. The design of the dynamic similarity relationships for the model soil and the corresponding preparation method can be refered to Wu et al.(2020). Accordingly, the density similarity ratio S_ρ and the shear modulus similarity ratio S_G of the model soil were determined to be 1/2.5 and 1/40, respectively. In the present study, resonant column tests were conducted on model soils with different mix proportions, and a final mass ratio of sawdust to sand of 1:2.5 was selected. The material parameters of the prototype strata and the model soil are listed in Table 2.

Table 2. Soil similitude parameters

	Density (kg/m^3)	Shear modulus (MPa)
Prototype Soil	1940	146.8
Idealized model soil	776	3.67
Actual model soil	791	3.60

2.4 Instrumentation

Within the model structure, accelerometers A1-A3 are installed on the floor in the three segments at the elevation of the ground surface, and the accelerometers A3-A6 are installed at the elevation of the structural base slab, as illustrated in Figure 5. Ten accelerometers (AS1 to AS10) are aligned as a matrix in the two observation planes, namely section 1-1 and section 2-2, and are installed 375 mm away from the model hub structure.

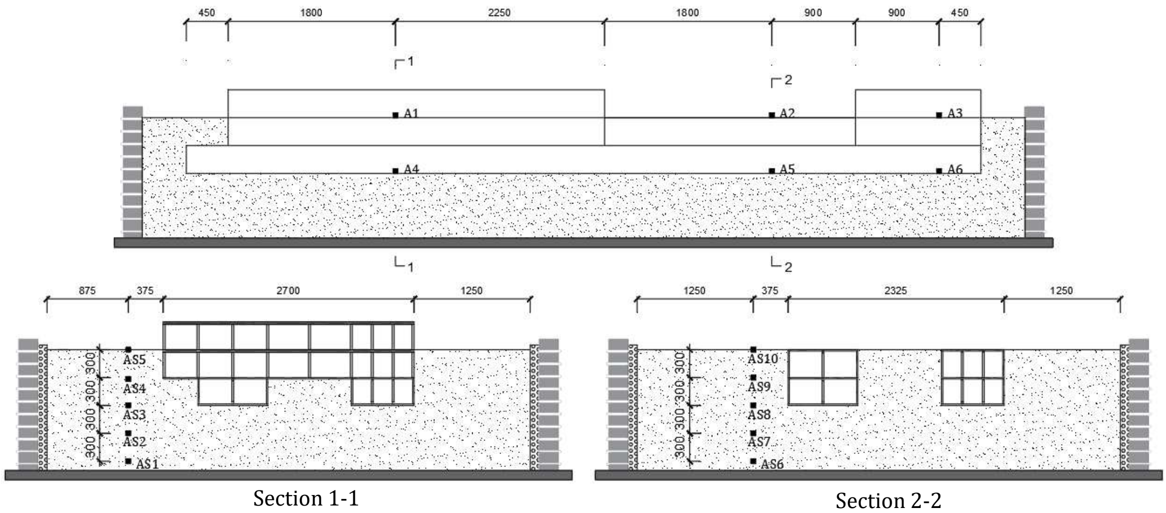

Figure 5. Layout of sensors

2.5 Seismic excitation

Based on the seismic fortification category of the prototype and the safety evaluation criteria of the engineering site, bedrock acceleration inputs corresponding to 63% and 10% probability of exceedance in a 100-year reference period were adopted in the experiment, with peak accelerations of 0.064 g and 0.16 g, respectively. Owing to the lack of recorded earthquake motions at the site, artificially synthesized seismic waves were selected as the acceleration inputs. The duration of the input ground motions was adjusted according to the time similarity ratio. The time-history curves and Fourier spectra of the artificially synthesized seismic waves used in the experiment are shown in Figure 6. The seismic excitation was applied in the transverse direction, as shown in Figure 1.

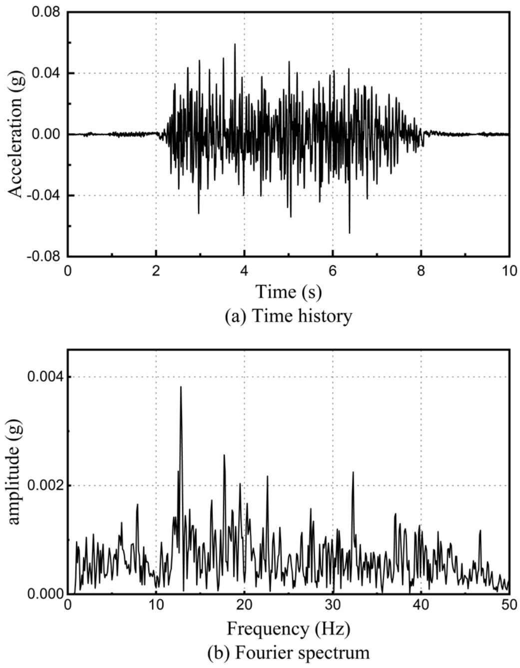

Figure 6. Time history and Fourier spectrum of input artificial ground motion

3 RESULTS OF THE SHAKING TABLE TESTING

3.1 Fundamental frequency of the model ground

The acceleration transfer function is introduced to identify the fundamental frequency of the model ground. The transfer function is defined as:

$$TF = \frac{FA_{response}}{FA_{input}}$$

where $FA_{response}$ is the Fourier amplitude of the acceleration response at the instrumentation points; and FA_{input} is the Fourier amplitude of the input motion in the White-Noise case. The transfer functions for different depths are plotted in Figure 7. The results indicate that the fundamental frequency of the model ground is 10.4 Hz. Furthermore, within the two soil acceleration monitoring sections, the fundamental frequencies obtained at all measurement points are identical, consistently equal to 10.4 Hz, demonstrating a high degree of uniformity of the model ground. Such a uniform ground condition effectively excludes the influence of soil heterogeneity on the dynamic response characteristics of the integrated structural system, thereby enabling a more rigorous and reliable assessment of the intrinsic response behavior of the integrated structure itself.

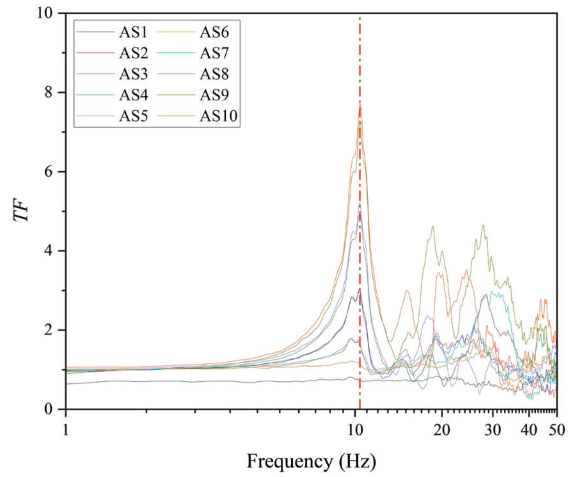

Figure 7. Acceleration transfer functions at different depths

3.2 Acceleration response of the model structure

The time-history curves of the acceleration responses in different structural segments at the ground surface elevation are plotted in Figure 8. The results show that the peak acceleration response in the station segment is smaller than those in the GTC and T3 segments. The acceleration response in the T3 segment is approximately 150% of that in the station segment. This demonstrates that, under seismic excitation, the vibration of above-ground structures imposes additional dynamic effects on the connected underground structures, thereby amplifying their seismic responses. Consequently, the dynamic responses in the segments connected to above-ground structures are markedly stronger than those in the segment of purely underground station.

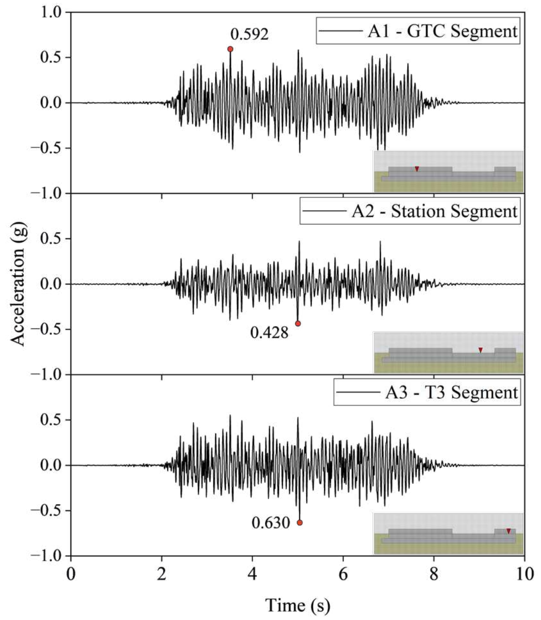

Figure 8. Acceleration time-history responses at the ground surface elevation

Figure 9 presents the acceleration responses at the elevation of the base slab with a burial depth of 0.6m. However, there are only minor discrepancies among the peak acceleration responses of the measurement points, indicating that the acceleration responses are generally consistent in different structural segments. The soil acceleration response at the burial depth of 0.6m was further extracted, and the Fourier spectral ratios between the response of the three structural segments and that of the surrounding ground were calculated. The results are presented in Figure 10. It can be observed that the Fourier spectral ratios are close to 1, indicating that the structure and the surrounding soil exhibit consistent spectral response characteristics.

This indicates that, at this depth, the structure and the surrounding soil exhibit consistent spectral response characteristics. These findings further demonstrate that the dynamic response in the base slab region of the underground station has not been significantly influenced by the vibration of the overlying structures, and that its seismic response is still predominantly governed by the shear strain characteristics of the surrounding soil.

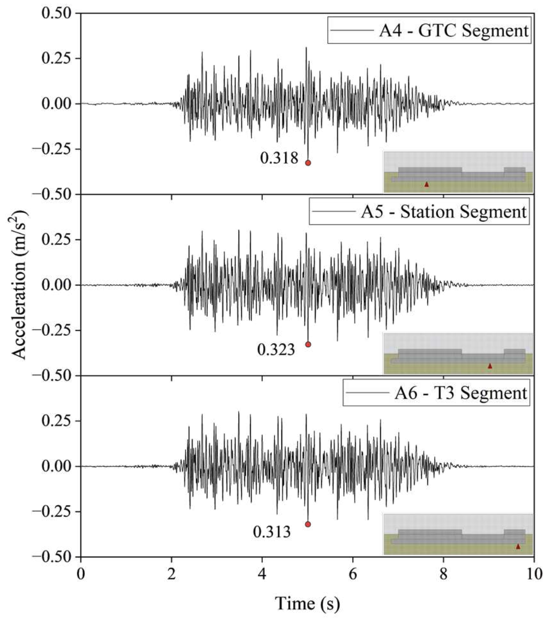

Figure 9. Acceleration time-history responses at the base slab elevation

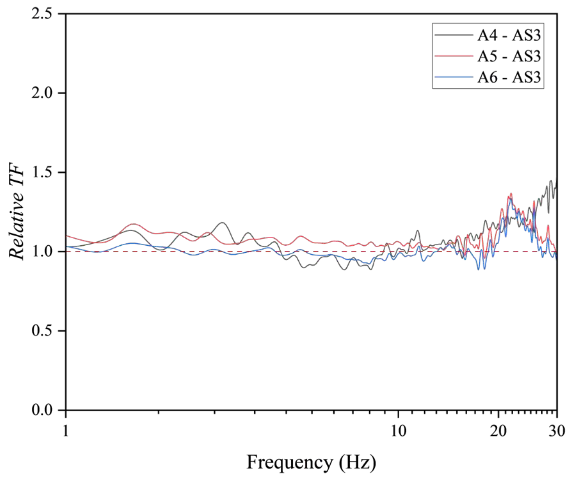

Figure 10. Fourier spectral ratios between the structure and the surrounding soil

3.3 Inter-story relative displacement

Inter-story displacement directly reflects the relative deformation between different sections of a structure and serves as an important engineering indicator for evaluating the seismic performance of underground structures. To further investigate the dynamic deformation characteristics of the underground station component within the integrated structural system, the time-domain integration method was employed to obtain the displacement time histories of the station roof slab and base slab in different segments. The inter-story displacement was defined as the relative horizontal displacement between the roof slab and the base slab in the same direction. Under the excitation of an artificial seismic wave with a peak acceleration of 0.16 g, the inter-story displacement time-history responses of the station platform level are shown in Figure 11.

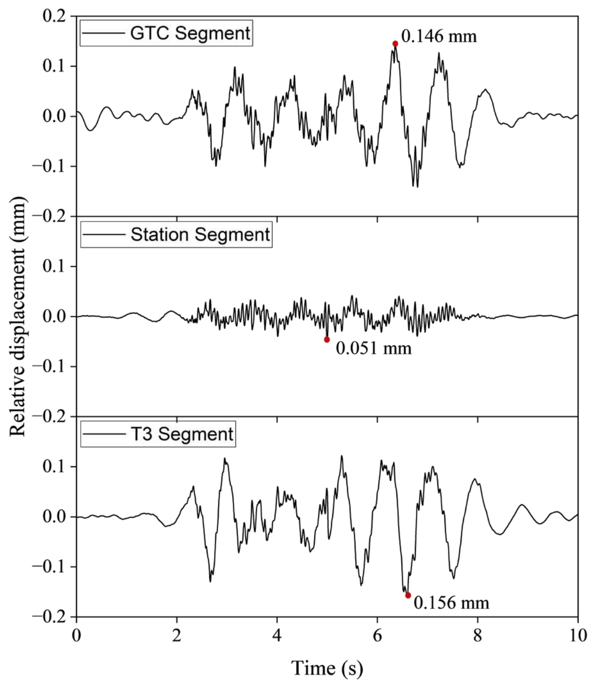

Figure 11. Inter-story displacement responses of the model structure

The results indicate that, within the underground station level, the inter-story displacement responses in the GTC segment and the T3 segment remain significantly larger than those in the station segment. In particular, the peak inter-story displacement in the T3 segment is approximately 3.1 times that of the station segment. These findings demonstrate that the presence of above-ground structures can markedly amplify the inter-story displacement response of the underground rail transit facility.

4 CONCLUSIONS

In this study, a large-scale shaking table test was conducted to investigate the seismic response characteristics of an integrated transportation hub system comprising underground stations and aboveground structures. The acceleration and inter-story displacement responses were systematically analyzed. The main conclusions can be summarized as follows:

1. The model ground exhibits a consistent fundamental frequency of 10.4 Hz at different depths in both ground acceleration monitoring sections, indicating uniform dynamic characteristics of the model ground.

2. Under transverse seismic excitation, the GTC and T3 segments exhibit more pronounced acceleration responses than the station segment. This is primarily attributed to the dynamic vibration of the aboveground structures, which induces amplification of the seismic responses in the corresponding underground components.

3. As the burial depth increases, the acceleration responses of the underground station components in different segments become essentially consistent. Moreover, the spectral characteristics of the underground station closely match those of the surrounding ground, indicating that the response of the underground station remains predominantly governed by the shear motion of the site.

4. From a deformation perspective, the GTC and T3 segments exhibit significantly larger inter-story displacements than the station-only segment. The peak inter-story displacement in the T3 segment reaches approximately 3.1 times that of the station segment. These results suggest that, in seismic design, particular attention should be paid to the displacement demands of underground station sections connected to aboveground structures.

REFERENCES

Chen, Z., Chen, W., Li, Y., & Yuan, Y. (2016). Shaking table test of a multi-story subway station under pulse-like ground motions. *Soil Dynamics and Earthquake Engineering*, 82, 111-122. http://doi.org/10.1016/j.soildyn.2015.12.002

Cheng, Y., Pan, D., Chen, Q., Huang, Y., & Zhang, D. (2023). Shaking table test on underground structure-soil-aboveground structure interaction. *Tunnelling and Underground Space Technology*, 140, 105300. http://doi.org/10.1016/j.tust.2023.105300

Li, W. T., Wang, R., & Zhang, J. M. (2023). Influence of aboveground structure on connected underground structure seismic response within an integrated system. *Tunnelling and Underground Space Technology*, 134, 105003. http://doi.org/10.1016/j.tust.2023.105003

LIN Gao, ZHU Tong, and LIN Bei. (2000). Similarity Technique for Dynamic Structural Model Test. *Journal of Dalian University of Technology*, 40(1), 1-8. (in Chinese)

Liu, R., Chen, Y., Wu, J., Xu, T., Gao, L., & Zhao, X. (2018). Mapping spatial accessibility of public transportation network in an urban area–A case study of Shanghai Hongqiao Transportation Hub. *Transportation research part D: transport and environment*, 59, 478-495. http://doi.org/10.1016/j.trd.2018.01.003

Qiu, D., Wang, P., Ren, W., Chen, J., & Zhao, C. (2023). Seismic responses and failure mechanism of the superstructure-integrated underground structure considering the seismic aboveground-underground interaction. *Soil Dynamics and Earthquake Engineering*, 175, 108259. http://doi.org/10.1016/j.soildyn.2023.108259

Tsinidis, G. (2017). Response characteristics of rectangular tunnels in soft soil subjected to transversal ground shaking. *Tunnelling and Underground Space Technology*, 62, 1-22. http://doi.org/10.1016/j.tust.2016.11.003

Wu, W., Ge, S., Yuan, Y., Ding, W., & Anastasopoulos, I. (2020). Seismic response of subway station in soft soil: Shaking table testing versus numerical analysis. *Tunnelling and Underground Space Technology*, 100, 103389. http://doi.org/10.1016/j.tust.2020.103389

Wu, W., Ge, S., Yuan, Y., Ding, W., & Anastasopoulos, I. (2021). Seismic response of a cross interchange metro station in soft soil: Physical and numerical modeling. *Earthquake Engineering & Structural Dynamics*, 50(9), 2294-2313. http://doi.org/10.1002/eqe.3446

Yuan, Y., Wang, Q., Liu, T., Yu, H., & Anastasopoulos, I. (2025). Seismic Response of Ground Penetrating Shield Tunnels Under Lateral Harmonic Excitations: Insights From Shaking Table Test. *Earthquake Engineering & Structural Dynamics*, 54(3), 867-884. http://doi.org/10.1002/eqe.4284